Available online at www.sciencedirect.com
SCIENCE DIRECT®
Microelectronic Engineering 78–79 (2005) 106–111
MICROELECTRONIC ENGINEERING
www.elsevier.com/locate/mee

Dry release fabrication and testing of SiC electrostatic cantilever actuators

Liudi Jiang [a,*], M. Hassan [b], R. Cheung [a], A.J. Harris [b], J.S. Burdess [c], C.A. Zorman [d], M. Mehregany [d]

[a] School of Engineering and Electronics, Scottish Microelectronics Centre, The University of Edinburgh, King's Buildings, West Mains Road, Edinburgh EH9 3JF, UK
[b] School of Electrical, Electronics and Computer Engineering, University of Newcastle Upon Tyne, Newcastle NE1 7RU, UK
[c] School of Mechanical and Systems Engineering, University of Newcastle Upon Tyne, Newcastle NE1 7RU, UK
[d] Department of Electrical Engineering and Computer Science, Case Western Reserve University, Cleveland, OH 44106, USA

Available online 30 December 2004

Abstract

This paper presents a simple, dry etching-based surface micromachining technique for the fabrication of single-layer polycrystalline 3C–SiC electrostatic actuators. The technique has utilized a single inductively coupled plasma recipe to etch and release metal patterned SiC structural layers. To demonstrate the simplicity of the process, SiC cantilever actuators with different beam lengths have been successfully fabricated using this method. By applying a combination of ac and dc voltages, the fabricated devices have been electrostatically actuated. The fundamental resonance frequencies of fabricated cantilevers with different lengths have been observed to range from 66.65 KHz to 1.729 MHz. The amplitudes of the fundamental resonance peaks with respect to the excitation voltages have also been systematically studied.

Keywords: SiC actuator; Inductively coupled plasma; Fundamental resonance frequency

1. Introduction

Silicon carbide (SiC) is a leading semiconductor material for devices designed for extreme operating conditions due to a unique collection of properties such as a large band gap, large breakdown field, great hardness, high wear resistivity, excellent thermal conductivity and chemical inertness. Because of these properties, SiC is an excellent candidate for microelectromechanical systems (MEMS) for use in harsh environments such as high temperatures, high wear and corrosive media where silicon MEMS are incapable [1].

* Corresponding author. Tel.: +44 131 6505610; fax: +44 131 6507475.
E-mail address: liudi.jiang@ee.ed.ac.uk (L. Jiang).

0167-9317/$ - see front matter
doi:10.1016/j.mee.2004.12.015

A host of surface machined SiC MEMS devices, such as mechanical resonators [2] and micromotors [3] have recently been demonstrated as a result of significant advancements in SiC deposition and patterning processes. In each of these cases, the devices were fabricated on SiO_2 and polycrystalline silicon (poly-Si) sacrificial layers, and released using aqueous etchants such as HF and KOH. Wet releasing procedures increase the risk of stiction, make batch process more challenging and greatly restrict the use of metal layers on the suspended structures.

In this paper, a novel surface micromachining technique that utilizes a single inductively coupled plasma (ICP) etching recipe to pattern and release the SiC structure layers is presented. The dry release step avoids the deleterious effects of surface tension that are often associated with wet release and also enables the use of metal coatings on the structural layers both as etch mask and as part of the electrodes. The process has been used to fabricate nichrome (NiCr) coated SiC cantilevers that could be electrostatically actuated by applying voltages between the top NiCr/SiC electrode and bottom substrate electrode.

2. SiC actuator fabrication

Single-layer SiC cantilevers have been fabricated using the process sequence shown in Fig. 1. The starting substrates consisted of 3-μm thick poly-Si films deposited by low pressure chemical vapour deposition on thermally oxidized Si wafers of 100 mm diameter. The thickness of the thermal oxide was nominally 1.5 μm. The poly-Si film acted as sacrificial layer and the SiO_2 film served as an insulating layer when applying electrostatic actuation. Polycrystalline SiC (poly-SiC) with a (1 1 0) texture has then been grown to a thickness of 2 μm using a two-step, carbonization-based, atmospheric pressure chemical vapour deposition process described in detail elsewhere [4]. Following the growth of the poly-SiC film, the wafers have been lightly polished using a silica-based slurry, ultrasonically cleaned in acetone and isopropanol,

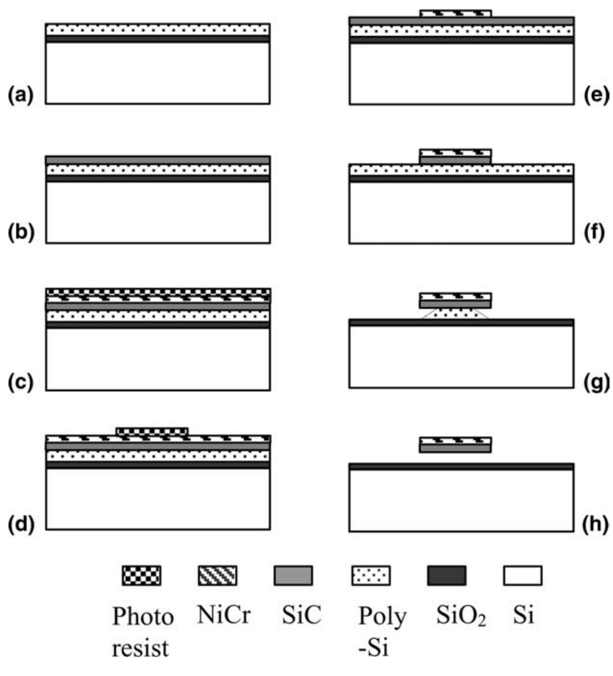

Fig. 1. Schematic diagram of the processing steps to fabricate SiC electrostatic cantilever actuators.

and then dipped in a HCl:H_2O (1:1) solution to reduce surface roughness and remove adventitious contamination. A 250-nm thick NiCr layer to be used as a SiC etch mask has then been deposited onto the SiC surface by thermal evaporation (Edwards Auto306). Following the NiCr deposition, a photoresist (Megaposit SPR2-2FX 1.3) layer has been spun on the NiCr film and photolithographically patterned into cantilever shapes. The cantilever patterns had widths of 15 μm and lengths of 25, 50, 100, 150, and 200 μm. The patterned wafers have then been exposed to a NiCr etchant (NiCr etchant TFC from Transene Company, Inc.) for an optimal time which was sufficient to remove the unmasked NiCr film as well as minimize the undercut to the formed patterns. In order to investigate the contact properties between the NiCr and SiC layers, NiCr pads have also been formed on the SiC layers along with the cantilever structures.

Following the NiCr patterning step, the poly-SiC films have been etched in inductively coupled SF_6/O_2 plasma that was optimized for both SiC and Si etching. The optimised conditions were 40 sccm SF_6 and 10 sccm O_2, 5 mT work pressure, 1000 W ICP coil power and 50 W chuck power, which correspond to a dc bias of about 100 V. The patterned NiCr was used here as etching mask. This SF_6/O_2 plasma first etched the SiC layer highly anisotropically because of the dominance of the ion-induced etch mechanism [5] and then continued to etch the poly-Si sacrificial layer underneath highly isotropically [6]. The undercut step finally released the cantilevers and formed suspended cantilever structures. Under these conditions, the etch rate selectivity of SiC to NiCr exceeded 60, which ensured the preservation of NiCr layer atop the patterned SiC layer upon completion of the ICP etch step. During this procedure, a SiC etch rate of 270 nm/min and silicon etch rate of 4 μm/min have been found, which suggested the etch rate selectivity of poly-Si to SiC was about 15. This indicates that SiC could automatically act as an outstanding mask material during the undercut of the poly-Si. The high etch rate selectivity of poly-Si to SiC coupled with the highly isotropic nature of the poly-Si etch means that the same recipe could be used to pattern and release the SiC beams in a single, continuous process without damaging beams during the release period of the process. Figs. 2(a) and (b) show scanning electron microscope (SEM) images of released cantilever structures fabricated using the aforementioned process.

3. Theory for electrostatic actuation

The fabricated cantilevers can be considered to consist of two adjacent electrodes forming two plates of a variable capacitor. For such a structure, the cantilever constitutes the movable plate of the capacitor and its displacement is controlled by the voltage applied across the plates, namely the top NiCr/SiC and bottom bulk Si electrodes. In a small deflection range, simple parallel plate theory [7] can be applied to characterize the dynamic behaviour of an electrostatically actuated cantilever. The electrostatic force, $F_{\mathrm{electrostatic}}$, between

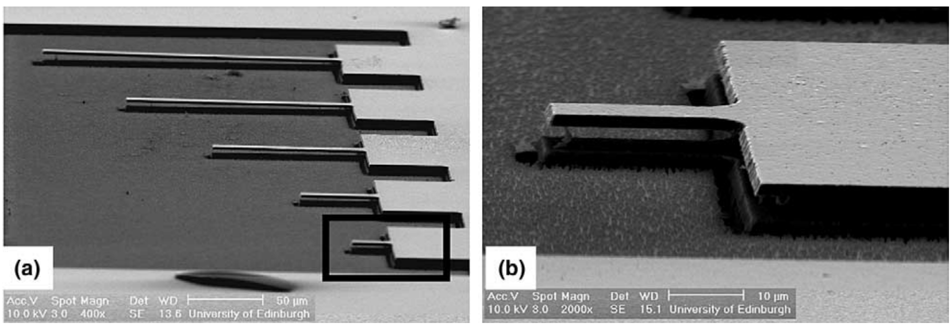

Fig. 2. (a) SEM micrographs of a group of cantilevers with varying lengths. (b) Enlarged image of the area indicated in (a).

the capacitor plates generated by applying a voltage V is

$$F_{\text{electrostatic}} = \frac{V^2 \varepsilon A}{2d^2} = kZ, \tag{1}$$

where ε is the permittivity in vacuum, d is the gap between the two electrodes, A is the area of one capacitor plate, k is the spring constant of the cantilever and Z is the amplitude of deflection due to V. It is obvious from this equation that amplitude $Z \propto V^2$.

For an ac voltage with a dc component, the square of the voltage is

$$\begin{aligned} V^2 &= (V_{\text{ac}} \sin \omega t + V_{\text{dc}})^2 \\ &= 2V_{\text{ac}}V_{\text{dc}} \sin \omega t + 0.5V_{\text{ac}}^2(1 - \cos 2\omega t) \\ &\quad + V_{\text{dc}}^2, \end{aligned} \tag{2}$$

where ω is the angular frequency of the applied ac voltage (V_{ac}).

It is obvious from the above equation that, only the first and second terms contribute to the resonance of the actuators. When the applied frequency of V_{ac} is chosen to be a fundamental resonance frequency (f_0) of the cantilevers, namely $\omega = 2\pi f_0$, only the first term can drive actuators into resonance at f_0. In contrast, when the applied frequency of V_{ac} is chosen to be $f_0/2$ ($\omega = \pi f_0$), only the second term can result in a fundamental resonance at f_0.

It is also worth noticing that the driving voltage and thereby the amplitude of the fundamental resonance peaks is related to $2V_{\text{ac}}V_{\text{dc}}$ and $0.5V_{\text{ac}}^2$, when $\omega = 2\pi f_0$ and πf_0, respectively.

4. Test results and discussion

In order to investigate the contact properties of the interface between the NiCr and SiC layers, *I–V* measurements using a standard two-point probe method have been carried out on the SiC surface both before and after NiCr deposition. The *I–V* characteristics are shown in Fig. 3. It indicated that, although Schottky behaviour was observed in Fig. 3(a) when electrically probing the uncoated poly-SiC layer, ohmic contact was achieved in Fig. 3(b) when NiCr metallization was used by thermal evaporation. Ohmic contact was required at the interface of NiCr/SiC as rectifying contact can create a dc component from a pure ac voltage and therefore influence the voltage and frequency characteristics of the actuators, as in Eqs. (1) and (2).

In order to determine their fundamental resonance frequencies, the fabricated SiC cantilever actuators have been subjected to extensive dynamic mechanical test by attaching them to a piezoelectric disc and vibrating them in a vacuum system. The dynamical actuation of the cantilevers was achieved through the piezoelectric disc which has been driven from a swept sine source. These experiments have been performed using an experimental set-up detailed elsewhere [8,9]. Using this mechanical method, the fundamental resonance

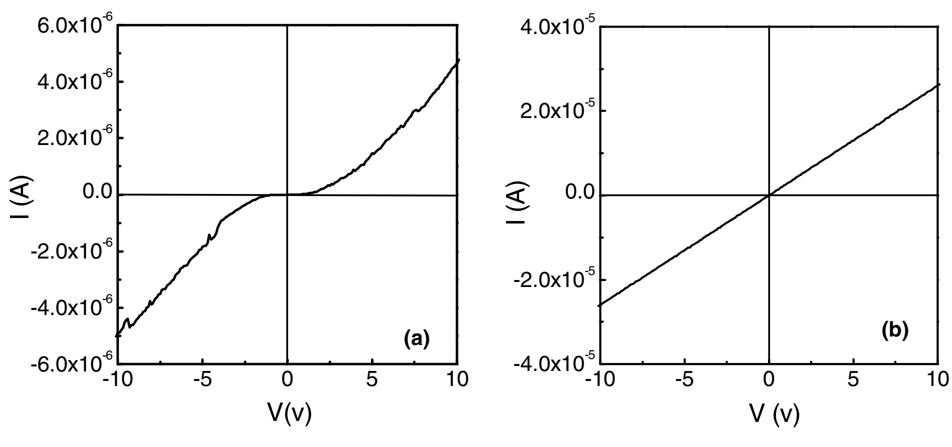

Fig. 3. *I–V* characteristics of: (a) a SiC surface before NiCr deposition, (b) after NiCr evaporation.

frequencies f_0 of the cantilevers could readily be determined and are listed in Table 1.

The electrostatic performance of the actuators have been characterised by applying a combination of a sinusoidal ac voltage (V_{ac}) and a dc (V_{dc}) voltage between the top NiCr/SiC and bottom bulk Si electrodes. The actuators have been excited electrostatically and the vibration of the beams as a function of frequency has been detected using an optical vibrometer (Polytec OFV 3001). The applied frequencies of the ac voltages have been chosen to be f_0 and $f_0/2$, respectively, where f_0 was obtained from the dynamical measurements described above. Since the cantilevers with different lengths behaved in similar way during the test, we only present here the results from the cantilevers of 200-μm long (f_0 = 66.65 KHz). Figs. 4(a) and (b) show observed fundamental resonance peaks for a 200-μm long cantilever excited by electrostatic actuation when the applied ac actuation

Table 1
Dynamically detected fundamental resonance frequencies of the fabricated SiC cantilever beams using vibration of a piezoelectric disk for actuation

Cantilever length (μm)	25	50	100	150	200
Frequency (Hz)	1.729 M	868.5 K	254 K	116.6 K	66.65 K

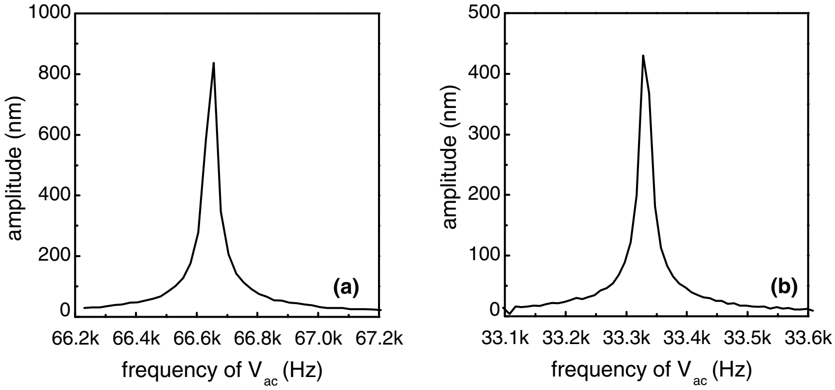

Fig. 4. Fundamental resonance peaks for a 200 μm long cantilever obtained when the applied ac frequency was (a) 66.65 KHz (V_{dc} = 0.6 V, V_{ac} = 0.2 V) and (b) 33.325 KHz (V_{ac} = 0.5 V).

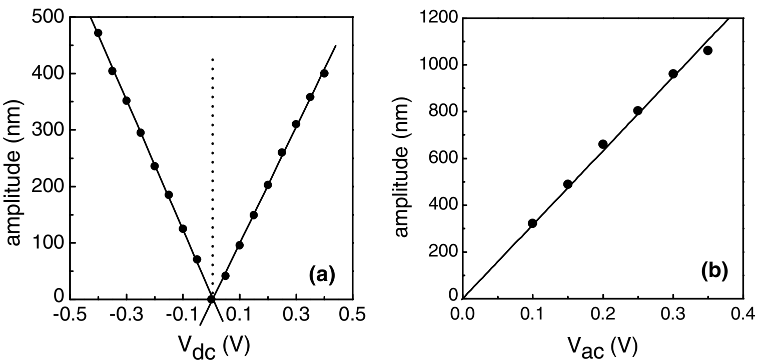

Fig. 5. Amplitude Z for a 200-μm long cantilever as a function of: (a) V_{dc} (V_{ac} = 0.3 V), and (b) V_{ac} (V_{dc} = 0.2 V). The frequency of the applied ac signal was 66.65 KHz. The solid lines are linear fits to the data points.

frequency was 66.65 (f_0) and 33.325 KHz ($f_0/2$), respectively. Linear relationships between the amplitude and the applied V_{dc} and V_{ac} components have also been detected when the ac voltage was applied at 66.65 KHz (f_0) and are shown in Figs. 5(a) and (b), respectively. These results are in agreement with the expected performance of electrostatic actuators as determined by Eqs. (1) and (2) in Section 3.

5. Conclusions

Polycrystalline 3C–SiC electrostatic actuators have been fabricated using a surface micromachining process that utilized one-step ICP dry etching process to pattern and release SiC device layers. This process has taken advantage of the anisotropic characteristic of the SiC etching and the isotropic etching nature of the poly-Si sacrificial layer. Patterned NiCr has been used both as hard mask during the ICP etching and electrode material for the fabricated actuators. The electrostatic actuators have been successfully excited by applying a sinusoidal ac voltage with a dc component at the fundamental resonance frequency f_0 and applying only a sinusoidal ac voltage at $f_0/2$. It has also been observed that the amplitude Z of the fundamental resonant peaks of the cantilevers changed linearly with applied V_{ac} and V_{dc}, respectively. These results confirmed that the electrostatic actuation of the cantilevers has taken place.

Acknowledgements

This work was supported by Engineering and Physical Sciences Research Council (EPSRC) Grant No. GR/R38019/01. We are grateful to A. Garrie for his help with the thermal evaporation of NiCr.

References

[1] M. Mehregany, C.A. Zorman, N. Rajan, C.H. Wu, Proceedings of the IEEE 86 (1998) 1594.
[2] S. Roy, R.G. DeAnna, C.A. Zorman, M. Mehregany, IEEE Transactions on Electron Devices 49 (2002) 2323.
[3] A.A. Yasseen, C.H. Wu, C.A. Zorman, M. Mehregany, IEEE Electron Device Letters 21 (2002) 2323.
[4] C.A. Zorman, S. Roy, C.H. Wu, A.J. Fleischman, M. Mehregany, Journal of Materials Research 13 (1998) 406.
[5] N.O.V. Plank, M.A. Blauw, E.W.J.M. van der Drift, R. Cheung, Journal of Physics D: Applied Physics 36 (2003) 482.
[6] Liudi Jiang, R. Cheung, M. Hassan, A.J. Harris, J.S. Burdess, C.A. Zorman, M. Mehregany, Journal of Vacuum Science and Technology B 21 (2003) 2998.
[7] M. Napoli, B. Bamieh, K. Turner, IEEE Proceedings of the 2003, in: American Control Conference, Denver, CO, June 4–6, 2003, 5 (2003) 3732.
[8] J. Hedley, A.J. Harris, J.S. Burdess, M.E. McNie, SPIE Proceedings on Design, Test and Packaging of MEMS/MOEMS 4408 (2001) 402.
[9] J.S. Burdess, A.J. Harris, D. Wood, R.J. Pitcher, D. Glennie, Journal of Microelectromechanical Systems 6 (1997) 322.